TECHNICAL TRANSACTIONS 8/2019
MECHANICS
DOI: 10.4467/2353737XCT.19.085.10864
SUBMISSION OF THE FINAL VERSION: 2/07/2019

Aleksander Kuranowski orcid.org/0000-0002-1688-7027
aleksander.kuranowski@mech.pk.edu.pl
Faculty of Mechanical Engineering, Cracow University of Technology

Electrical power steering – modelling and bench testing

Elektryczne urządzenie wspomagające kierownicę – modelowanie i badania stanowiskowe

Abstract

The article presents a dynamic model of an electric device supporting the steering system of a passenger car; the model was verified through a series of bench tests. The research object was an integrated electric power steering system (EPS) mounted on a steering column and cooperating with a steering gear. The results of the theoretical analysis were compared with the results of tests performed on a specially built research bench fully reflecting the work of assistance in the car. A satisfactory level of agreement between the results of the model tests and the bench tests was obtained.

Keywords: EPS, modelling, bench tests

Streszczenie

W artykule przedstawiono zweryfikowany testami laboratoryjnymi dynamiczny model elektrycznego urządzenia wspomagającego kierownicę. Przedmiotem badań było zintegrowane elektryczne urządzenie wspomagające kierownicę (EPS) zamontowane na kolumnie kierownicy. Wyniki analizy teoretycznej porównano z wynikami testów przeprowadzonych na specjalnie zbudowanym stanowisku badawczym w pełni odzwierciedlającym pracę urządzenia w samochodzie. Uzyskano zadawalającą zgodność między wynikami badań stanowiskowych a wynikami analiz teoretycznych.

Słowa kluczowe: EPS, modelowanie, stanowisko badawcze

1. Introduction

The subject of this work is the development of an EPS device model and its verification with the results of bench tests. Workplace tests of an electrically supported passenger car steering system were conducted in order to determine the values of the stiffness, damping and friction parameters occurring in the assistance system. Harmonic measures were applied from the steering wheel and wheels.

The study of the EPS system includes the examination of both the control objectives and the control strategies. Control objectives relate to the size of the support system and to the feeling of the road. Control strategies are divided into classic strategies resulting from the drive automation and strategies using models developed separately.

The article [5] focuses on the development of a control algorithm and analyses the choice of simplifications applied when developing a control system to approximate the mechanical characteristics of a vehicle.

Articles [7, 9] present a simulation of the EPS control system integrated with the overall dynamic vehicle model. Co-simulation was used, i.e. the simultaneous cooperation of two software environments (ADAMS and Matlab) by means of a subprogram specifying data channels and running the ADAMS environment in each simulation clock. Using co-simulation, a multi-mass dynamic model of a vehicle cooperating with the EPS control algorithm was simulated on the smooth road with one inequality [7]. The author of article [9] presented a method of modelling the EPS system and its co-simulation in combination with the control system. The mechanical model was calibrated using the experimentally measured torsional stiffness of the torsion bar and the friction of the mechanism. The EPS model optimised in ADAMS was converted into Matlab/Simulink, and was then combined with the Simulink driver model. Co-simulation was performed and described for the frequency response test of the EPS device. The proposed method enables a good prediction of the dynamics of the EPS system and can be an effective way to optimise the EPS control system.

The authors of article [8] proposed two indicators – steering sensitivity and road feel – in order to assess the performance of the steering system. It was found that steering sensitivity depends on the following factors: stiffness of the torque sensor, the electrical characteristics of the propulsion engine, its moment of inertia, the transmission ratio of the power steering, the boost control and the vehicle parameters.

In [1], the authors considered the possibility of adjusting steering sensitivity; they used a simplified model of the steering system, containing both a reduced mechanical and an electrical model. The effectiveness of the adopted simplification has been proven by computer simulation.

Of the many methods of torque control of an electric motor used in EPS systems, the authors of article [2] drew attention to the method of selecting the moment consisting of minimising the difference between the values of the standard moment and the measured moment. The process of designing a controller which realises the algorithm of minimising the mentioned difference is presented. During the tests, the discontinuity of the steering torque was analysed due to the fact that this moment occurs both with and without assistance. It has

been *surmised* that the cause of discontinuity is the occurrence of dry friction in the steering system. After formulating the requirements for the steering torque controller by specifying the target values for the characteristic parameters of the control device, a H_∞ type controller was developed which was implemented as a steering torque controller using frequency--dependent weighted functions.

2. Model of the EPS support device

Figure 1 shows an EPS device that has been removed from the vehicle and connected to the rack steering gear, and Fig. 2 shows the dynamic model of the system.

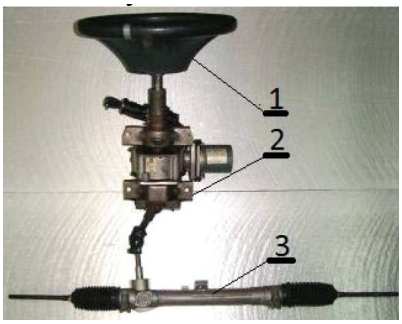

Fig. 1. The actual steering system with the electric assist device;
1 – steering wheel, 2 – EPS, 3 – steering gear

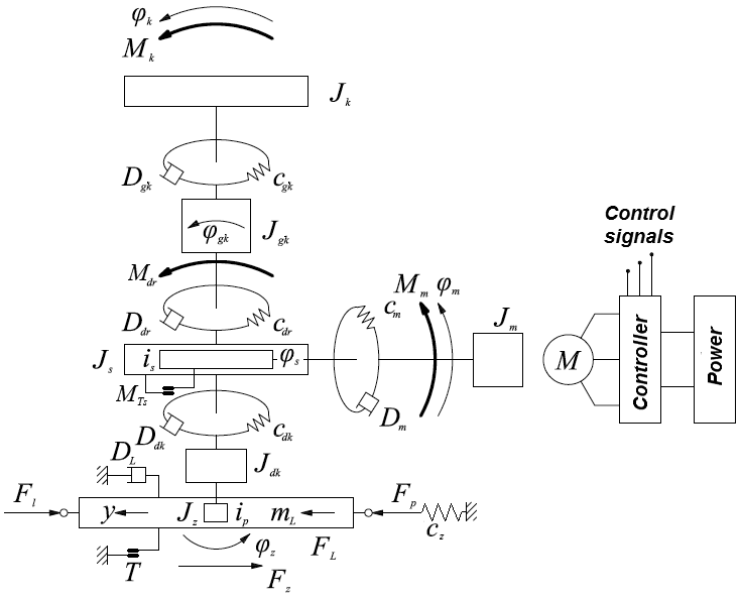

Fig. 2. The dynamic model of a steering system with electric assist device

Notation:

c_{dk} – angular stiffness of the lower part of the column
c_{dr} – angular stiffness of the torsion bar
c_{gk} – angular stiffness of the upper part of the column
c_{m} – angular stiffness of the electric motor clutch
c_{z} – stiffness of the elastic housing of the rack
D_{dk} – damping factor the lower part of the steering column
D_{dr} – damping factor of the torsion bar
D_{gk} – damping factor of the upper part of the steering column
D_{L} – damping factor of the rack
D_{m} – damping factor of the electric motor
F_{L} – external force of the steering rods imported from the axle rack
F_{l} – force in the left tie rod
F_{p} – force in the right tie rod
F_{z} – circumferential force on the pinion gear
i_{p} – steering gear ratio
i_{s} – worm gear ratio
J_{dk} – moment of inertia of the lower part of the column
J_{gk} – moment of inertia of the upper part of the column
J_{k} – moment of inertia of the steering wheel
J_{k+d} – moment of inertia of the steering wheel including mass of the hand
J_{m} – moment of inertia of the rotor of the electric motor
J_{s} – moment of inertia of the worm wheel
J_{z} – moment of inertia of the pinion
k_{e} – electromechanical constant
k_{ws} – constant assisted
M_{dr} – torque occurring on torsion rod
M_{k} – torque applied to the steering wheel
M_{m} – the electric motor torque assist device
M_{Ts} – friction torque of the worm gear
m_{L} – mass of the rack
T – friction force of the rack
y – shift of the rack
φ_{dk} – angle of rotation of the lower section of the steering column
φ_{gk} – angle of rotation of the upper part of the column
φ_{k} – angle of rotation of the steering wheel
φ_{m} – angle of rotation of the electric motor
φ_{s} – angle of rotation of the worm wheel
φ_{z} – angle of rotation of the pinion

The equations of the system dynamics shown in Fig. 2 are recorded as follows:

$$J_k\ddot{\varphi}_k + D_{gk}\left(\dot{\varphi}_k - \dot{\varphi}_{gk}\right) + c_{gk}\left(\varphi_k - \varphi_{gk}\right) = M_k \tag{1}$$

In view of the kinematic forced rotation of the steering wheel it was assumed that $\varphi_k = \varphi_{gk}$.

$$J_s\ddot{\varphi}_s + c_{dr}\left(\varphi_s - \varphi_k\right) + c_{dk}\left(\varphi_s - \varphi_z\right) + c_m i_s^2\left(\varphi_s - \frac{\varphi_m}{i_s}\right) = 0 \tag{2}$$

$$J_m\ddot{\varphi}_m + c_m\left(\varphi_m - \varphi_s i_s\right) + M_{Tm} = M_m \tag{3}$$

$$\left(J_{dk} + m_l r_z^2\right)\ddot{\varphi}_z + D_l r_z^2\dot{\varphi}_z + c_{dk}\left(\varphi_z - \varphi_s\right) + Tr_z + c_z r_z^2\varphi_z = \left(F_p + F_l\right)r_z \tag{4}$$

Damping of the rack described by the $D_l r_z^2\dot{\varphi}_z$ member was omitted. The engine torque depends on the stiffness and the angle of deflection of the torsion bar placed in series with the gear pinion described by constant k_{ws}:

$$M_m = k_{ws}c_{dr}\left(\varphi_k - \varphi_s\right) \tag{5}$$

Differential equations of motion of the booster are linear, thus it was possible to apply the principle of superposition. Therefore, differences in the variable waveforms with the power off and the variable waveforms corresponding to the system with the power on are caused by influence of unstable torque due to the introduction of additional torque of assist motor M_m. The numerical analysis results discussed later were verified experimentally on a specially built test bench.

The model of isolated steering system simulating the conditions of the bench measurements was formulated on the basis of the following assumptions:

- Sinusoidal kinematic input function caused changes of the angle φ_k of the steering wheel rotation with amplitude ±15° and frequency 0.5 Hz.
- External loading of the system is caused by the deformation of the spring elements having a coefficient of stiffness c_z connected in series with the gear rack.
- Assist torque from the electric motor is proportional (P-controller) to the torsional moment on the torsion bar mounted on the steering column.
- Friction forces are described using the model of Coulomb.
- Omitted from the model are:
- the impact of universal joints;
- flexibility of the rack gear housing;
- play in the moving joints;
- dynamics of the control system (sensors, transducers).

The mechanical model of the analysed system had three degrees of freedom: φ_k; φ_m; φ_z. Differential equations describing the dynamics of the system were solved in Matlab. As in [3], the torque of the EPS electric motor was treated as the product of the current i and the electromechanical constant k_e.

$$M_m = k_e \cdot i \tag{6}$$

Values of the parameters of the examined model are shown in Table 1.

Table 1. Values of the parameters of the tested EPS model

Values that were determined	Notation	Value	Unit of measure
moment of inertia of the steering wheel	J_k	$33 \cdot 10^{-3}$	kgm^2
moment of inertia of the upper part of the column	J_{gk}	$4.62 \cdot 10^{-5}$	kgm^2
moment of inertia of the worm wheel	J_s	$0.83 \cdot 10^{-3}$	kgm^2
moment of inertia of the rotor of the electric motor	J_m	$0.0321 \cdot 10^{-3}$	kgm^2
moment of inertia of the lower part of the column	J_{dk}	$0.002 \cdot 10^{-3}$	kgm^2
moment of inertia of the pinion	J_z	$5.48 \cdot 10^{-6}$	kgm^2
angular stiffness of the upper part of the column	c_{gk}	9800	Nm/rad
angular stiffness of the torsion bar	c_{dr}	91	Nm/rad
angular stiffness of the electric motor clutch	c_m	3.85	Nm/rad
angular stiffness of the lower part of the column	c_{dk}	2400	Nm/rad
stiffness of the elastic housing of the rack	c_z	$1.7 \cdot 10^6$	N/m
damping factor of the upper part of the steering column	D_{gk}	0.0275	Nms/rad
damping factor of the torsion bar	D_{dr}	0	
damping factor of the electric motor	D_m	0.0035	Nms/rad
damping factor the lower part of the steering column	D_{dk}	0	
damping factor of the rack	D_L	0.0275	Ns/m
worm gear ratio	i_s	0.0455	
steering gear ratio	i_p	20.5	rad/m
mass of the rack	m_L	1.45	kg
friction force of the rack	T	175	N

3. Workplace tests

A steering system with a rack gear and an EPS supporting device was installed on a special measurement and research stand (Fig. 3). The advantage of this is stand is that it was created from the deconstruction of this part of the CAN communication, which is essential in cars for the operation of steering assistance. The amount of assistance was dependent upon the set driving speed. Two types of steering rotation were generated.

In the first type of steering rotation (test I), a direct-current (DC) motor with two different rotational speeds was used to drive the steering wheel, allowing a steady rotation

of the steering wheel. The input torque was transferred to the steering column via a worm gear and a toothed belt. This enabled testing at two rotational speeds of the steering wheel: 0.2 rpm and 0.4 rpm. The drive system of the steering wheel was equipped with circuit breakers in order to protect against overload resulting from the extreme positions of the rack. These breakers allowed the reversible operation of the stand with steering wheel rotation in the range of ±500°.

In the second type of extortion (test II), harmonic kinematic exclusion was first performed from the steering wheel side and then from the rack side using a connecting rod machine originally used to determine the characteristics of the shock absorbers. This machine was powered by a 40 kW DC motor. Variable stroke adjustment in the range of 0–100 mm and smooth regulation of the frequency of excitation were possible. The uniformity of the drive was ensured by the flywheel with an inertia moment of 17.0 kgm^2.

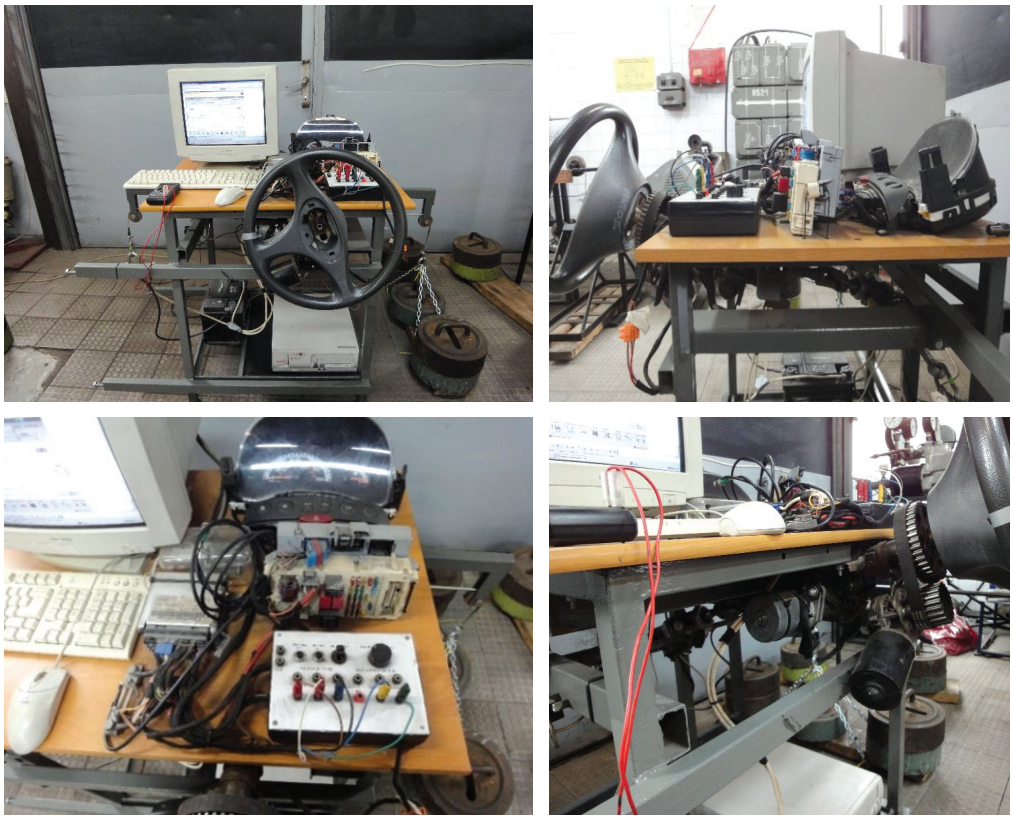

Fig. 3. View of the test bench for the EPS device with equipment

Measurements of forces and displacements were performed by equipping the stand with additional external devices, specifically, HBM force sensors and wire sensors to measure displacements (turn of the steering wheel, shift of the rack).

Table 2. Listing of external measuring equipment

Sensor type	Type	Measurement range	Accuracy
force sensor	HBM U2B	20 kN	±0.02%
position sensor	Kubler DB3A1	500 mm	±0.1%

For the driver's input function, the steering wheel was connected to the machine connecting rod fastener using a 1.5-m-long connector with ball joints. The wire sensors were used to measure the angle of rotation of the steering wheel and the displacement of the toothed bar. The cable for measuring the angle of the rotation of the steering wheel was wound on a wheel mounted on the steering column shaft, which was coaxial with the steering wheel.

At the input function from the side of the steering wheel, the load on the rack was obtained by elastic elements of a stiffness, connecting the gear rack to the housing.

3.1. Tests of the input function of the steering wheel

Two types of tests were performed on the input function of the steering wheel:

- rotation of the steering wheel by an angle of ±500°,
- harmonic excitation in the range of ±15°.

During tests with a steering wheel rotation of ±500°, the transmission worked without a load and the steering wheel rotation was at one of two values: either the speed of around 0.2 rpm or 0.4 rpm.

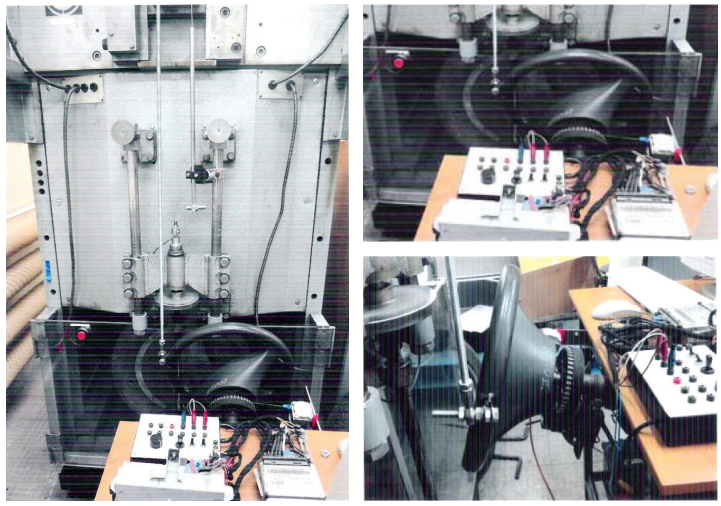

Fig. 4. Bench tests with harmonic input function from the steering wheel in the range of ±15°

Taking into account the transmission ratio of the rack gear, the harmonic input function of the steering wheel caused the displacement of the rack by approx. 2.5 mm. The investigations concerned two cases: a free (unloaded) rack; a rack supported by elastic elements with a stiffness of around $1.7 \cdot 10^6$ N/m.

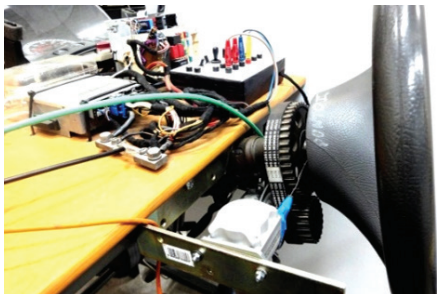

Fig. 5. Work bench tests with kinematic input function on the steering wheel side within the range of ±500° rotation

The bench tests included measurements of the torque at a ±15° steering wheel rotation in which the movements of the steering wheel are performed during the correction that takes place during the process of driving.

In order to determine the torque developed by the motor M_m at different booster operating states, the characteristics $M_k = {}_f(\varphi_k)$ were first determined with the booster switched off, followed by the same input parameters (amplitude $\varphi = \pm 15°$ and frequencies f = 0.5, 1.0, 1.5 Hz) with the assistive device switched on.

The constructed test stand proved to be sufficiently functional and the registered characteristic curves showed repeatability.

3.2. Tests at the input function from the rack

The tests of the steering system at the kinematic input function of the gear rack movement were performed on the modernised stand (Fig. 6).

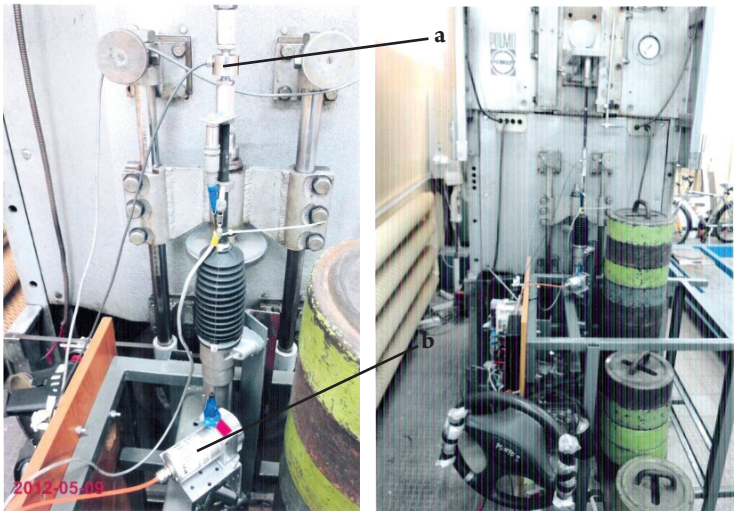

Fig. 6. Research on kinematic input function from the rack mounted in a vertical position; a – force sensor, b – position sensor

The adaptation of the stand consisted of the articulated connection of the gear rack with the machine slider for, among other purposes, testing the shock absorbers using the steering rod (with factory ball joints) on which the force sensor was mounted. The amplitude of the input function had a fixed value of ±15 mm. Such a displacement of the rack caused rotation of the steering wheel in the range of approximately ±175°. The frequency of the input function excitation was either 0.1 or 1.0 Hz.

The tests concerned transmission with an assistance mounted with different loading of the system: free steering wheel without additional weight; steering wheel loaded on the circumference with weight 0.8 kg multiplied by 2, replacing the weight of the driver hand and forearms placed freely on the steering wheel.

A very strong dependence of the dynamic load of the rack on the size of additional masses attached to the steering wheel was observed. In the case of the steering wheel without additional weight, the force in the rack did not exceed 0.75 kN. There were noticeable vibrations related to the torsional elasticity of the torsion bar. With mounted masses of 0.8 kg multiplied by 2, and a similar kinematic input function – the force loading the sprocket increased around four times up to nearly 3 kN.

3.3. Comparison of the results of bench and simulation tests

Two simulation tests were performed.

Test I referred to forcing the rotary-oscillating motion of the steering wheel with a sinusoidal waveform and is described by the following parameters: frequency of input function 0.5 Hz, the absence of a load on the side of the rack ($c_z = 0$), and simulated car speed of 0 km/h. Figure 7 shows the time courses of changing the angle of rotation of the steering

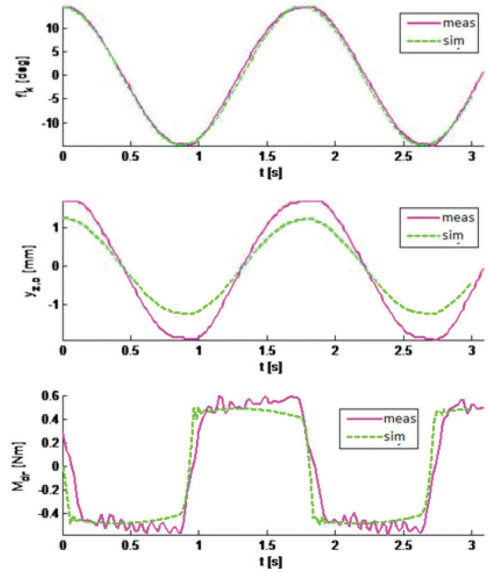

Fig. 7. Comparison of time courses from bench measurements and simulations during Test I

wheel φ_k and the displacement of the rack relative to the housing $y_{z,o}$. Figure 8 presents the torque courses of the torsion bar M_{dr} equal to the torque at the steering wheel M_k.

When forcing a change in the angle φ_k with a sinusoidal pattern, the occurring displacement of the rack $y_{z,0}$ is similar and only slightly changed by the friction forces at the extreme positions. A smaller displacement of the $y_{z,o}$ racks was obtained with the model in comparison with the bench tests. The mapping of moment changes of the M_{dr} torsion bar is satisfactory with regard to the phase and amplitude of the response, although according to the model, the changes do not show vibrations at the vertices of the waveform. The above statements are also confirmed by the torque characteristics as a function of the angle of rotation of the steering wheel, which is shown in Fig. 8.

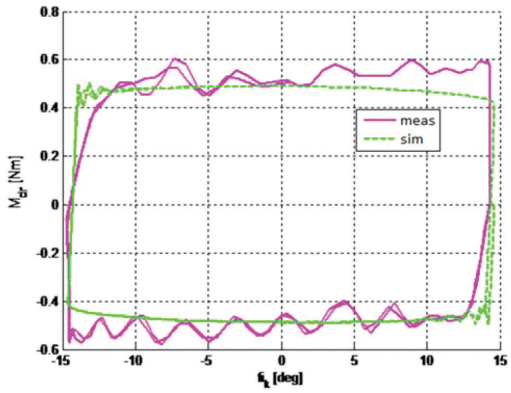

Fig. 8. Comparison of example runs from bench measurements and simulations of torque changes on the steering wheel $(M_{dr} = M_k)$ as a function of the angle of rotation of the steering wheel

Test II consisted of forcing a rotational-oscillating motion of the steering wheel with a sinusoidal waveform, where the frequency of input function is 0.5 Hz, loads on the side of the rack with stiffness $c_z = 1.7 \cdot 10^6$ N/m, and the simulated car speed = 0 km/h. Figure 9 shows the changes of the steering wheel rotation angle φ_k, the displacement of the rack with respect to the housing, $y_{z,o}$ and the moment of the M_{dr} torque rod equal to the torque at the M_k steering wheel.

Due to an applied sinusoidal input function, φ_k moves along a similar course as $y_{z,o}$, which is slightly deformed by friction forces in extreme positions. In the model's response, a smaller amplitude of displacement of the $y_{z,o}$ racks was obtained. The mapping of torque changes on the M_{dr} torsion bar is satisfactory with regard to the phase and amplitude of the response, although the variables determined through the use of the model do not show interference at extreme positions.

Details of the results obtained from the model in the form of a torque graph as a function of the angle of rotation of the steering wheel are shown in Fig. 10.

The waveforms of the variables determined by the model are satisfactorily represented in relation to the hysteresis loop width and the average slope of the characteristic, although this is not very similar to the S-letter profile. The linear course without accentuating the S-letter

profile can be explained by the linear dependence of the torque of the auxiliary motor from the steering angle of the control rod with the torque value assumed in the model. In fact, as research shows, the dependence is not linear and it is progressive.

The adopted simulation model of the electrical booster satisfactorily describes the real object despite the introduced simplifications. There is a noticeable influence of friction, which causes a hysteresis loop effect with a width similar to the previously measured one. The vibrations, which are small but noticeable at higher frequencies in the study, are not true to a simulative mapping. It could be caused by the irregular torque of the DC motor.

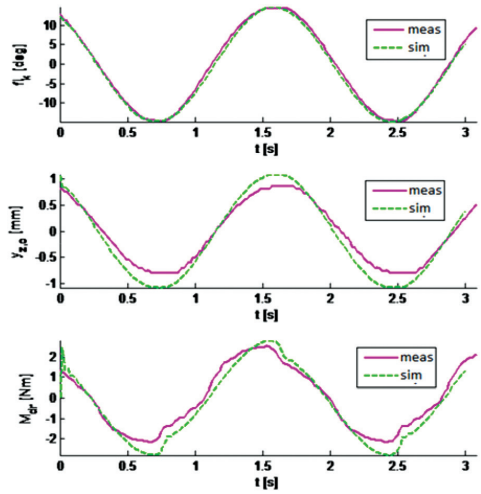

Fig. 9. Comparison of time courses from bench measurements and simulations during Test II

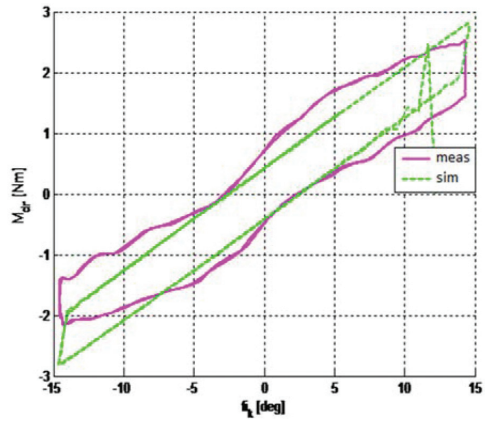

Fig. 10. Comparison of example runs from bench measurements and simulations of torque changes on the steering wheel ($M_{dr} = M_k$) as a function of the angle of rotation of the steering wheel

It can be assumed that a better representation of the actual characteristics of the transmission can be obtained if instead of the linear relationship between the torque of the motor and the load of the transmission, the non-linear function is introduced.

The EPS current characteristics were determined on the same bench. The waveform of changes in current values as a function of the torque on the steering wheel at different speeds is shown in Fig. 11. It was found that the value of EPS current as a function of the torque for an assumed velocity increases to a certain value in a non-linear manner, and after reaching the value imposed by the limiter, it is intentionally limited and takes an almost constant value.

The equation approximating a non-linear increase in the current can be written as:

$$I(M) = a \cdot M \cdot e^{b \cdot M} \tag{7}$$

where a, b, and e are parameters dependent upon speed.

Estimation of parameters a and b by the method of least squares at a confidence level of 95% enabled determining the function approximating the results of measurements in a range of non-linear dependence. Based on the measurements, it was assumed that in the range of linear dependence, the current is constant.

$$I(M) = const = c \tag{8}$$

Theoretical characteristics (Fig. 12) of the current intensity obtained at different speeds were similar to obtained results of the measurements (Fig. 11). Appropriate values of the parameters a, b and c were determined. The values of these parameters at speeds within the range of 0–160 km/h with increments of 20 km/h are shown in Table 3.

Table 3. Values of the parameters of the equation (8) describing the EPS current

v km/h	a	b	c
0	0.74	0.33	37.5
20	0.24	0.43	22.5
40	0.24	0.31	17.5
60	0.16	0.30	14.8
80	0.07	0.38	14.6
100	0.11	0.31	14.8
120	0.10	0.33	15.0
140	0.09	0.34	15.0
160	0.09	0.33	15.0

Figure 11 shows changes in the intensity of the current supplying EPS as a function of the torque on the steering wheel. Changes in the intensity of the EPS current as a function of the steering wheel torque when simulated at different driving speeds are shown in Fig. 12. On account of ensuring legibility of the drawing, the number of speeds plotted was limited to only six. Figure 13 shows changes in the intensity of the EPS supply current when the vehicle is at a standstill.

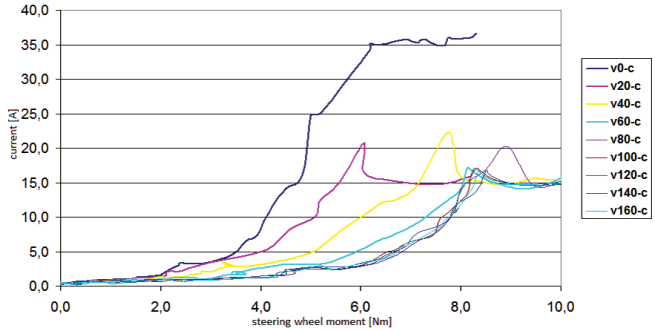

Fig. 11. Chart of assist-motor current intensity depending upon the steering wheel torque

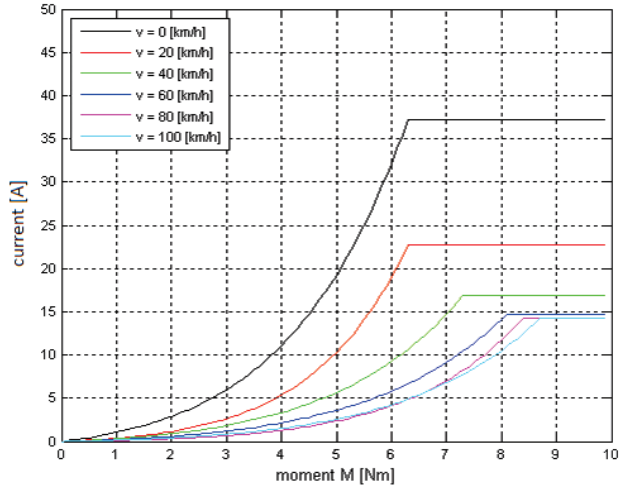

Fig. 12. Changes in EPS current intensity as a function of the torque on the steering wheel different speeds simulated on the bench

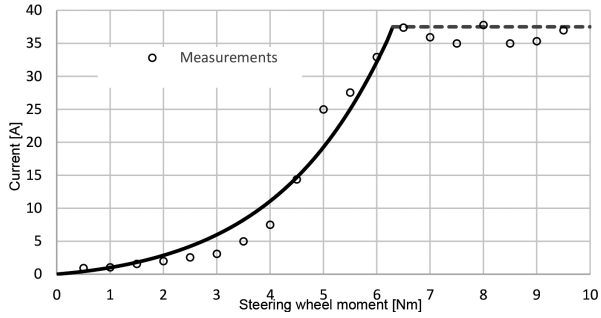

Fig. 13. Changes in current intensity as a function of the torque on the steering wheel; velocity $v = 0$ km/h

The method of controlling the current intensity as a function of the steering wheel torque and dependent upon the driving speed is shown in the spatial diagram (Fig. 14).

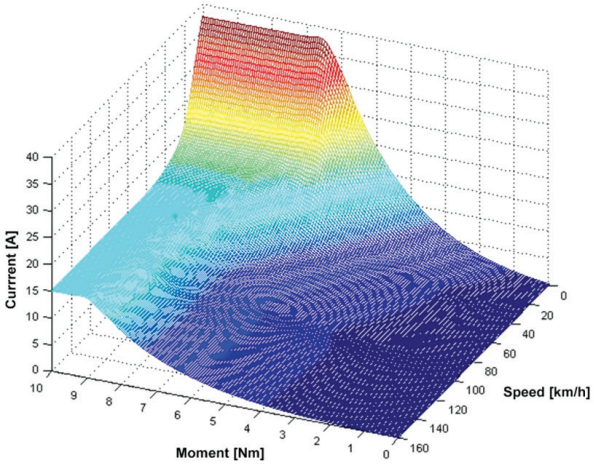

Fig. 14. Changes in EPS current intensity as a function of the torque on the steering wheel and variable speed

The torque developed by the engine of the booster is dependent upon the current value of the electromechanical constant, hence the fact that the shape of the shell $I = f(M_k)$ maps the shape of the support characteristic. The current intensity value is the resultant value of the EPS device controller and it determines the course of the characteristics.

4. Conclusions

Waveforms determined by the model are satisfactorily well represented in relation to the width of the hysteresis loop and the average slope of the characteristic (Fig. 10), again this seems very vague – you should clearly state which characteristic you are referring to although this does not demonstrate a clear similarity with the S-profile. The linear course without emphasising the S-profile can be explained by the linear dependence of the torque between the auxiliary motor and the steering angle controlling the torque value in the model. In fact, as this research shows, the dependence is not linear; it has a progressive character.

The adopted simulation model of the electrical booster, despite the introduced simplifications, satisfactorily describes the real object. There is a noticeable influence of friction, which causes a hysteresis effect with a width similar to the previously measured one. The vibrations, which are small but noticeable at higher frequencies in the study, are not true to a simulative mapping.

It can be assumed that a better mapping of the actual transmission characteristics can be obtained if instead of the linear relationship between the engine torque and the transmission load, a non-linear function is introduced.

The author is also an employee of the Institute of Forensic Research (Instytut Ekspertyz Sądowych im. prof. dra Jana Sehna).

References

[1] Badawy A., Zuraski J., Bolourchi F., Chandy A., *Modeling and Analysis of an Electric Power Steering System*, Delphi Automotive Systems 2009, 25–31.

[2] Dannöhl C., Müller S., Ulbrich H., *H_∞-control of a rack-assisted electric power steering system*, Vehicle System Dynamics 2011, 1–18.

[3] Data S., Pesce M., Reccia L., *Identification of steering system parameters by experimental measurements processing*, Proc. Instn. Mech. Engrs 218, Part D: J. Automobile Engineering 2004, 783–792.

[4] Govender V., Khazaridi G., Weiskircher T., Keppler D., Müller S., *A PID and state space approach for the position control of an electric power steering*, 16th Stuttgart International Symposium Automotive and Engine Technology, March 2016, 755–770.

[5] Kim J.-H., Song J.-B., *Control logic for an electric power steering system using assist motor*, Mechatronics 12, 2002, 447–459.

[6] Kuranowski A., *Effect of variable input and output on the characteristics of a steering system with EPS (Electric power system)*, Journal of KONES, 19, No. 1, Warszawa 2012, 215–226.

[7] Liao Y.G., Du H.I., *Cosimulation of multi-body-based vehicle dynamics and an electric power steering control system*, Proc. Instn. Mech. Engrs. 215, Part K, 2001, 141–151.

[8] Liu Z., Yang J., Liao D., *The Optimization of Electric Power Assisted Steering to Improve Vehicle Performance*, Proc. Instn. Mech. Engrs. 217, Part D, 2003, 639–646.

[9] Qiu Y., *Electrical power steering mechanical modelling and co-simulation with control system*, Institute of Sound and Vibration Research University of Southampton, 2010.

[10] Xue-Ping Z., Xin L., Jie Ch., Jin-Lai M., *Parametric design and application of steering characteristic curve in control for electric power steering*, Mechatronics 19, 2009, 905–911.

If you want to quote this article, its proper bibliographic entry is as follow: Kuranowski A., *Electrical power steering – modelling and bench testing*, Technical Transactions, Vol. 8/2019, pp. 143–158.